Geomorphology 299 (2017) 24–38

Contents lists available at ScienceDirect

Geomorphology

journal homepage: www.elsevier.com/locate/geomorph

Constraints on the Miocene landscape evolution of the Eastern Alps from the Kalkspitze region, Niedere Tauern (Austria)

Florian Dertnig [a,*], Kurt Stüwe [a], Jon Woodhead [b], Finlay M. Stuart [c], Christoph Spötl [d]

[a] Institute of Earth Sciences, University of Graz, Heinrichstraße 26, 8010 Graz, Austria
[b] School of Earth Sciences, The University of Melbourne, Vic. 3010, Australia
[c] Isotope Geosciences Unit, Scottish Universities Environmental Research Centre, Scottish Enterprise Technology Park, East Kilbride G75 0QF, UK
[d] Institute of Geology, University of Innsbruck, Innrain 52, 6020 Innsbruck, Austria

ARTICLE INFO

Article history:
Received 31 March 2017
Received in revised form 16 September 2017
Accepted 20 September 2017
Available online 28 September 2017

Keywords:
Landscape evolution
Cave levels
U-Pb dating
Cosmogenic ^{21}Ne dating

ABSTRACT

In order to unravel aspects of the Miocene landscape evolution of the eastern European Alps, we present geomorphic and isotopic data from the western Niedere Tauern region (Austria). The region is critical for such interpretations, because it is one of the few regions along the topographic axis of the Eastern Alps where the highest peaks (up to 2500 m a.s.l.) are dominated by limestone. As such, the region contains a record of Miocene landscape-forming events that survived the Pleistocene glaciations, not preserved elsewhere in the central Eastern Alps. This record includes karst caves, karstified planation surfaces and crystalline fluvial pebbles (Augenstein Formation) preserved on planation surfaces and in karst caves. Caves in the region occur in three distinct levels that correlate with well-known cave levels in the Northern Calcareous Alps, although they are somewhat higher in the Niedere Tauern. In part, these cave elevations also correlate with three planation surfaces and knickpoints of major streams draining the region, testifying their pre-glacial origin. We report details of a karst cave (Durchgangshöhle) from the highest cave level located at 2340 m a.s.l. In this cave, allochthonous fluvial gravels are present, overgrown by speleothems. One speleothem yielded an early middle Pleistocene U-Pb age (682 ± 17 ka). We regard this as a minimum age for the erosion of the fluvial cave deposits during Marine Isotope Stages 17 or 16. Carbon and oxygen isotope data of these speleothems imply a climate that is consistent with this interpretation. Cosmogenic ^{21}Ne data of fluvial quartz clasts collected from the surface on plateaus of the Northern Calcareous Alps suggest minimum exposure durations of 115 and 262 ka. They probably reflect successive exposure since removal of the sediment cover of the Oligocene Augenstein Formation during the Pleistocene. While our geochronological data fail to record aspects of the earlier Miocene uplift history, they are consistent with the overall geomorphic history inferred from the geomorphic markers. This suggests that the Niedere Tauern share a common uplift history with the Northern Calcareous Aps and implies a moderate south-north topographic gradient that has been maintained since the Miocene.

1. Introduction

The onset of surface uplift and relief building in the Alps in the Miocene is a subject of intense debate (Frisch et al., 1998; Kuhlemann, 2007; Champagnac et al., 2009; Willett, 2010; Hergarten et al., 2010; Wagner et al., 2011). Unfortunately, geomorphological observations are of limited use for this discussion, because large parts of the Eastern Alps were repeatedly glaciated during the last two million years and glacial erosion obliterated many of the earlier landforms. The morphological interpretation of the Miocene landscape evolution is therefore largely confined to regions outside the Pleistocene glaciations (Legrain et al., 2015) or to Neogene features that survived glacial erosion (Montgomery and Korup, 2011; Sternai et al., 2012). One such feature are the fluvial siliciclastic gravels of the Augestein Formation, that occur on highly elevated plateaus in the Eastern Alps ("Augenstein landscape") (Fig. 1) (Winkler-Hermaden, 1957; Frisch et al., 2001). The Augenstein landscape is a feature inherent and largely limited to the karst system of the Northern Calcareous Alps (NCA). There, it has been used to infer the evolution of surface uplift in the Miocene (Frisch et al., 2001), but it remains questionable if this model also pertains to the evolution of the topographic axis of the orogen located some tens of kilometers further south. There, most evidence for uplift is only indirectly derived from rock uplift rates via low-temperature geochronological methods (Hejl, 1997; Reinecker, 2000). Given that the surface uplift history of an iconic mountain belt like the Alps is at the very heart of the quest to understand mountain-forming processes,

* Corresponding author at: Chair of Applied Geophysics, Montanuniversität Leoben, Peter-Tunner-Straße 25, 8700 Leoben, Austria.
E-mail addresses: florian.dertnig@unileoben.ac.at (F. Dertnig), kurt.stuewe@uni-graz.at (K. Stüwe), jdwood@unimelb.edu.au (J. Woodhead), Fin.Stuart@glasgow.ac.uk (F.M. Stuart), Christoph.Spoetl@uibk.ac.at (C. Spötl).

https://doi.org/10.1016/j.geomorph.2017.09.024
0169-555X/

it is therefore important to expand our knowledge of surface uplift in the NCA to the mountain range as a whole.

In this paper, we widen the potential of the peculiar Augenstein landscape for the interpretation of the geomorphological evolution of the Eastern Alps by investigating corresponding evidence in regions south of the NCA (Fig. 1), in the crystalline units of the central axis of the Eastern Alps. In order to discern the Augenstein deposits from other fluvial gravels in these regions, the Kalkspitze region of the Niedere Tauern range was selected where limestone constitutes the topographically highest elevations (Fig. 2). This region features the rare occurrence of karstifiable rocks at the main divide of the Eastern Alps. Importantly, the region also features planation surfaces, karst caves and other geomorphic elements that have not been investigated in detail. We compare cave systems to levels within the overall fluvial system (see Harmand et al., 2017) and provide a comparison of the Niedere Tauern range to the NCA to the north in order to present an integrated surface uplift history for the central Eastern Alps as a whole.

2. Geological background

Kalkspitze is part of the main divide of the Eastern Alps in the Niedere Tauern range and consists of karstified low-grade metamorphic limestones and other carbonates that belong to different tectonic units. In the following we refer to the karst region as the Western Niedere Tauern (WNT) (Figs. 1, 2).

The WNT region is located on the watershed of the Eastern Alps between the west-east striking Salzach and Enns valleys to the north and the Mur valley to the south (Fig. 2b). The highest peaks along the divide are Steirische Kalkspitze (2459 m), Lungauer Kalkspitze (2471 m) and Hochgolling (2862 m) in the Schladminger Tauern, some 20 km to the east. To the west, the divide continues into the Tauern Window (Fig. 1), where peaks commonly rise up to above 3000 m including Austria's highest mountain, Grossglockner (3798 m). The Dachstein massif to the north of the Enns valley also reaches almost 3000 m in elevation. South to north and north to south flowing streams that drain the WNT from the divide towards the Salzach/Enns and Mur valley systems, respectively, form 10–20 km-long glacially carved U-shaped valleys. At high elevations, the WNT forms a glacio-karst landscape featuring a large number of small lakes.

Tectonically, Kalkspitze and the bulk of the WNT are part of the Austroalpine nappe complex with a Mesozoic tectonic history and first relief evolution in the early Oligocene. The WNT directly overlies the Penninic Tauern Window some 20 km to the south and west of Kalkspitze (Schmid et al., 2004). Within the WNT, the Austroalpine is subdivided into the Lower Austroalpine and the Upper Austroalpine of the Schladming Complex. North of the Schladming Complex (which includes Kalkspitze), the Greywacke Zone forms a narrow strip of soft metamorphosed Paleozoic sedimentary rocks along the Enns valley, which constitutes a major Miocene strike-slip fault system: the SEMP. The Dachstein massif north of the SEMP is part of the Mesozoic NCA. The SEMP fault separates the high relief of the NCA from the WNT and has been active during the Miocene landscape evolution (Decker and Peresson, 1996; Linzer et al., 1997; Wang and Neubauer, 1998; Keil and Neubauer, 2009; Bartosch et al., 2017).

The Kalkspitze region and much of the WNT are largely made up of Mesozoic carbonates (Fig. 2a). These rocks are coeval with the carbonate rocks of the NCA, but are of slightly higher metamorphic grade and degree of deformation (Schmid et al., 2004). Rocks of the Raibl Group (a mixed carbonate-siliciclastic unit within the Upper Triassic stratigraphy of the NCA) are interleaved as isolated pods within the carbonate rocks. The latter are underlain by the Lantschfeld quartzite, the dominant rock type between the Kalkspitze and the Enns valley to the north. Due to structural inversion during the Cretaceous nappe stacking events (Frisch, 1979; Ratschbacher, 1986), this quartzite also forms the very top 5 m of the Steirische Kalkspitze summit. The Schladming Complex to the east and south of Kalkspitze is mostly made up of para- and orthogneisses interleaved with amphibolites.

2.1. Landscape evolution

The history of rock- and surface uplift in the Eastern Alps is still incompletely understood. Sediment data from basins around the Alps (Kuhlemann et al., 2002) and numerical modeling studies (Hergarten et al., 2010) suggest an onset of surface uplift some 30 Ma ago. The central and eastern NCA provide good examples of prolonged rock- and surface uplift since the Neogene, in part because of the presence of distinct planation surfaces. These karst plateaus correlate with three discrete cave levels, traditionally referred to as the Ruin (2200 ± 300 m), Giant (1600 ± 500 m) and Source (800 ± 300 m) levels (Fischer, 1990; Frisch et al., 2002). Speleological studies demonstrate that each of these levels formed within the (epi-)phreatic zone at river base level. They therefore represent excellent markers of the surface uplift history (cf. Palmer, 1987). The age of these subhorizontal cave levels has been inferred to be Oligocene (Ruin level), lower Miocene (Giant level) and Pliocene to present (Source level) (Frisch et al., 2001), suggesting a stepwise rock- and surface uplift of the NCA since 30 Ma. The inferred age of the Ruin level is supported by the age of the Dachstein paleosurface which is located between 1800 m and 2500 m. This paleosurface contains crystalline pebbles considered to be remnants of a ~1.3 kilometer-thick fluvial sediment deposit (the Augenstein Formation) sourced by rivers from south of the SEMP during the Oligocene (Frisch et al., 2001). The crystalline pebbles of the Augenstein Formation are usually found in karst depressions and caves. Typically, they occur together with reddish paleosoils formed under a subtropical climate (Kuhlemann et al., 2008). A broad range of lithologies including polycrystalline quartz, quartzite, greenstone, acid volcanics, red sandstone, vein quartz and carbonate are described from these pebbles. While their Oligocene age assignment has yet to be confirmed, sediment successions of coarse material equivalent to the Augenstein deposits occur in the Molasse basin along the alpine front at distinct sediment fans. There, their Oligocene age is well established (Tollmann, 1968; Frisch et al., 1998, 2002). Sedimentation of Augenstein gravel was terminated by the onset of lateral extrusion and the formation of the Enns valley along the SEMP around 18 Ma (Ratschbacher et al., 1991; Frisch et al., 1998; Keil and Neubauer, 2011a; Bartosch et al., 2017).

The uplift history of the crystalline axis of the Eastern Alps is mostly only indirectly inferred from low-temperature geochronological studies. Fission-track ages for regions such as Koralpe and Gurk valley indicate that these regions were already exposed albeit at low elevation, around 52–31 Ma and 35–29 Ma, respectively. In contrast, the Schladming block appears to have only been exhumed around 23–14 Ma (Hejl, 1997; Reinecker, 2000). Fission-track and apatite (U—Th)/He data of Wölfler et al. (2012) indicate a more or less continuous exhumation of the Tauern Window and topography development of much of the region east of this window between 17 and 5 Ma (Herbst, 1985; Genser et al., 1996). Frisch et al. (2002) suggested that this surface uplift occurred somewhat earlier than in the NCA so that a topographic gradient from south to north (high to low) was maintained during much of the Miocene. At the eastern end of the Alps Wagner et al. (2011) and Legrain et al. (2014) recognized a surface uplift event that may have raised the eastern end of the Alps by up to 1 km in the last 4–5 Ma, but the effect of this event further west is unknown.

This uplift history appears to be intimately related to movements along the SEMP (Keil and Neubauer, 2015; Bartosch et al., 2017). The displacement along the SEMP is part of the lateral extrusion of the Eastern Alps and its activity peaked between 18 and 13 Ma, involving several tens of kilometers of sinistral strike-slip motion (Ratschbacher et al., 1991; Decker and Peresson, 1996; Linzer et al., 1997; Wang and Neubauer, 1998). South of the WNT, the Tamsweg intramontane basin

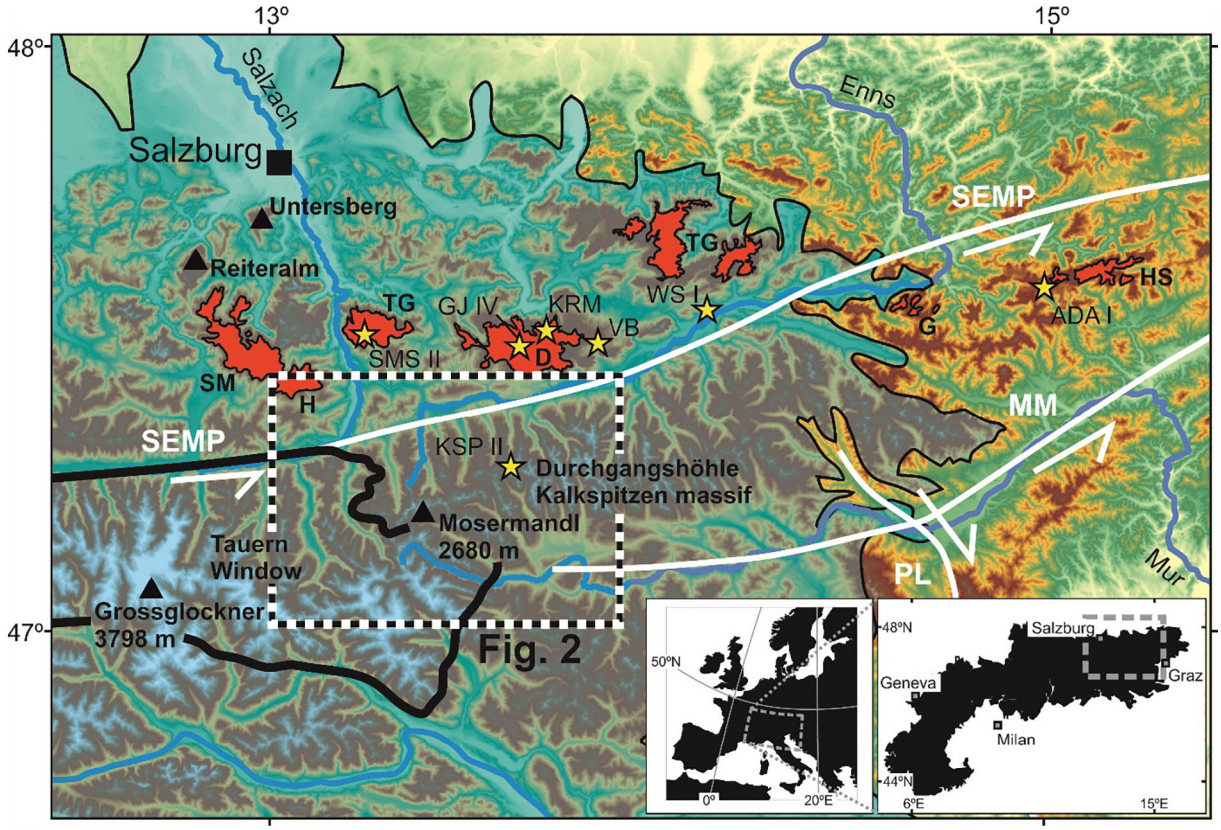

Fig. 1. Topographic map of the central and eastern segment of the Eastern Alps (insets show Europe and the Alps above 600 m elevation). The light blue overlay represents the maximum extent of the ice cover during the last glacial maximum (van Husen, 2000). Blue lines represent main rivers and white lines major fault systems: SEMP = Salzach-Enns-Mariazell-Puchberg fault; MM = Mur-Mürz fault; PL = Pöls-Lavanttal fault. Regions with Augenstein occurrences in the Northern Calcareous Alps above 1800 m a.s.l. are in red (from various sources, but mainly from Winkler-Hermaden, 1957): SM Steinernes Meer, H Hochkönig, TG Tennengebirge, D Dachstein, TG Totes Gebirge, G Gesäuse, HS Hochschwab. The black line delineates the Tauern Window. Locations of Augenstein samples analyzed for Ne isotopes (including sample labels) and the Kalkspitzen massif are marked by yellow asterisks.

formed at this time accommodating clastic sediments from low-elevation regions (Ratschbacher et al., 1991). Following the period of lateral extrusion, surface uplift may have proceeded continuously forming the lower cave levels in the NCA and raising the topography of the WNT region. During the Pleistocene glaciations the drainage networks were partly rearranged by overdeepening of the Enns valley and the WNT developed its present-day morphology (Keil and Neubauer, 2009).

In summary, it appears that Miocene exhumation and related tectonic processes occurred somewhat later and were more active south of the SEMP than in the NCA to the north. Conversely, surface uplift south of the SEMP appears to have preceded surface uplift of the NCA so that a continuous topographic south-north gradient was maintained during the Oligocene and Miocene (Frisch et al., 2002).

3. Morphological observations

In order to provide a more accurate comparison of the landscape evolution north and south of the SEMP, we report morphometric parameters obtained from digital elevation models and fieldwork. Planation surfaces and channel profiles were mapped and a number of caves were investigated.

3.1. Planation surfaces

Rather flat areas with shallow slopes on mountain shoulders and summit plateaus are abundant in the WNT region. These planation surfaces are typically between 1500 m and 2400 m (Figs. 2b, 3g) and can be divided into three distinct levels, some of which are too small to map on the scale of Fig. 2b. The highest level surface (~2400 m) is present only as isolated patches and can be found in the flat summit areas for example on Lungauer Kalkspitze and Glöcknerin (Figs. 3a, g). The intermediate level surface (~2200 m) is the most extensive, and includes areas adjacent to Akarscharte between the two Kalkspitze summits (Fig. 3a) and, more impressively, at Gasthofkar north of Mosermandl. This intermediate level also bears the largest abundance of dolines. The lowest level surface (~1600 m) is rather small (Fig. 4), constituting bulk of the rural areas to the north of the main divide. The lower planation surface is found within about 3 km of the SEMP in the north and the intermediate planation surface reaches as near as Speiereck (2411 m) in the south, towards the Mur valley (Fig. 2b). By the nature of the topography of the WNT, the regions north and south of the divide feature almost only the lower and intermediate planation surface levels, respectively. The highest level is mostly present along the divide itself. Overall, all the individual levels are difficult to distinguish as there are smooth transitions between them. This problem of planation surface distinction is largely due to widespread slope movements as shown e.g. by double ridges and rockfall.

3.2. Channel profiles

Channel profiles, reflecting neotectonics and landscape evolution, were investigated for rivers draining the divide of the WNT to the north and south towards the base levels of the Salzach (544 m near Bischofshofen), Enns (745 m near Schladming) and Mur (1022 m near Tamsweg) rivers (Fig. 5). Dedicated software (http://hergarten.at/geomorphology) and the SRTM 1 arc sec digital elevation model were used. Knickpoints of the rivers were identified as areas between linear

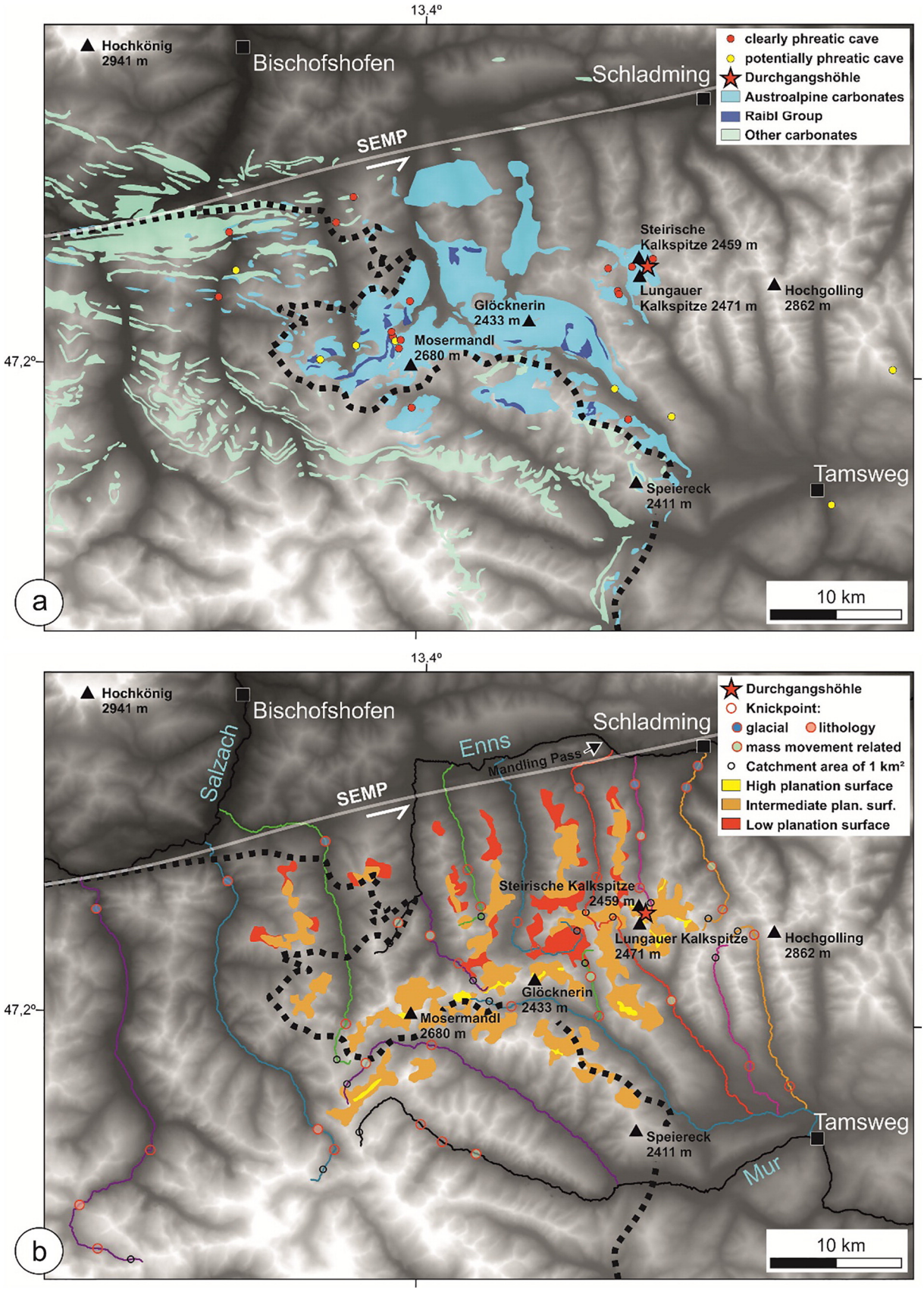

Fig. 2. Topographic map of the western Niedere Tauern (WNT) and the black dashed line delineates the Tauern Window. (a) Distribution of caves, carbonate rocks and other lithologies. (b) Planation surfaces mapped in this study. Color-coded rivers refer to channels profiles shown in Fig. 5.

data sections in the logarithmic steepness to area plot (e.g. Wobus et al., 2006). In particular, we investigated three channels draining into the Salzach, six channels that drain northwards into the Enns and another six channels that drain south into the Mur system (Fig. 2b). The morphometric characteristics and knickpoints of the three major base-level rivers were described by Robl et al. (2008). Further streams in and near the study region were analyzed by Keil and Neubauer (2009, 2011b). All three investigated tributaries of the Salzach (Gasteiner

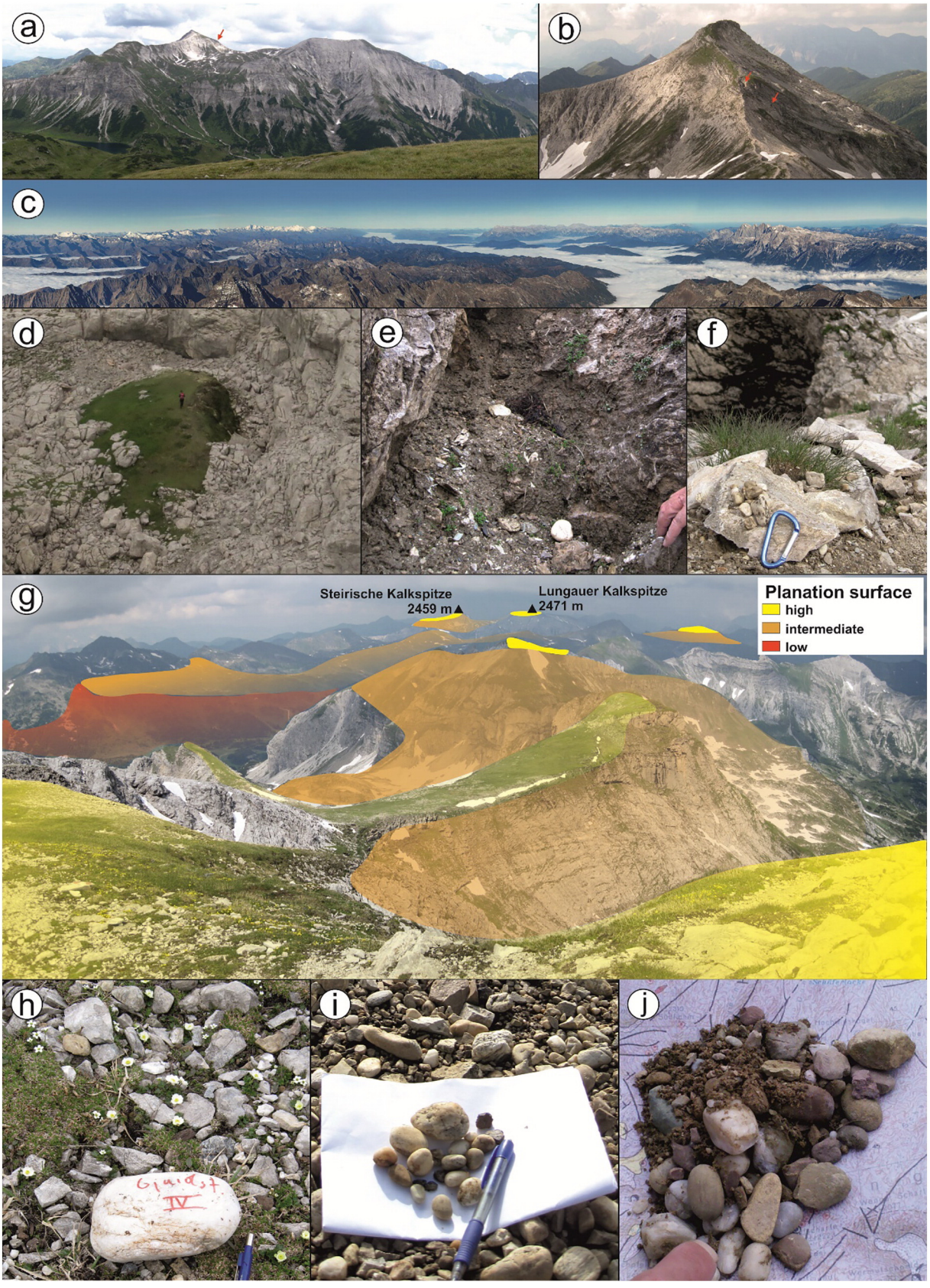

Ache, Großarl- and Kleinarlbach) show two to four distinct knickpoints along their profiles (Fig. 5a). As for all rivers draining into the Salzach between Zell am See and Bischofshofen, the three analyzed rivers feature a major knickpoint near their base level next to the SEMP fault (Fig. 5a) (forming the gorges of the Gasteiner and Lichtenstein Klamm), while higher knickpoints occur typically between 1100 m and 1800 m a.s.l.

The six rivers that drain to the Enns river are, from west to east, the Pleißlingbach, Taurach North, Zauchen-, Forstau-, Preunegg- and Ober-Talbach (Fig. 2). The channel profile of the Pleißlingbach is more graded than the other channels (Fig. 5b; no. 1). The Taurach North and Zauchenbach channel profiles feature knickpoints only in their upper reaches (Fig. 5b; no. 3, 4). In contrast to the eastern tributaries, the channel profiles of Forstau-, Preunegg- and Ober-Talbach (Fig. 5b; no. 5, 6, 7) have distinct knickpoints entering the Enns valley. Overall, these three rivers are defined by steep upper and flat lower reaches. Some knickpoints of the Enns catchment correlate either with areas of present or historic mass movements (Fig. 5b; no. 1, 2, 6, 7) (Braunstingl et al., 2005).

According to Robl et al. (2008) the Mur river has an overall graded channel profile, but a detailed analysis (this study) shows that a few minor knickpoints occur in its uppermost part of the WNT. All the tributaries of the Mur seem more graded than the north-flowing rivers (Fig. 5). However, there are knickpoints that can be correlated with mass movements, for example, the highest knickpoints of the Rieding-Zederhausbach and Taurach South, and the lowest of the Mur, Weißpriach- and Göriachbach (Fig. 5c; no. 1, 2, 4, 5, 7). The Taurach South features a knickpoint at the confluence with the Lantschfeldbach (Fig. 5c; no. 3, 4). Similar to the Enns catchment the channel profiles of the Mur tributaries Weißpriach-, Lignitz- and Göriachbach (Fig. 5c; no. 5, 6, 7) feature steep upper parts and shallow lower parts. Also similar to some of the north-flowing rivers, the lowermost knickpoint of two of these Mur tributaries the Weißpriach- and the Göriachbach correlate with mass movements (Fig. 5c, no. 5, 7).

3.3. Caves and other karst features

Caves and surface karst features occur in the WNT in a number of different sizes and abundance (Fig. 2a). 42 caves are registered in the Austrian cave cadaster for this region (Klappacher, 1992), most of which are within one of the carbonate units of the Tauern Window or the Austroalpine. Caves showing a vadose morphology or those located next to faults or folds were excluded from our considerations, because the morphology of these caves does not reflect the paleo-base levels. 25 caves of potentially phreatic origin were identified and used for further analysis. Most of these caves are only a few tens of meters long, but some comprise up to several hundreds of meters of passages (e.g., Durchgangshöhle). Several caves occur ~100 m below the summit of Steirische Kalkspitze, where the banded calcite marble (Bänderkalkmarmor) of Kalkspitze overlies dolomite marble of the Wetterstein Formation. Caves formed within both lithologies and Durchgangshöhle described below, is the largest in this line of caves. Although the total number of caves and the total cave passage length is small compared to those of the NCA, some statistics on their distribution were obtained by plotting the cumulative passage length against elevation (Fig. 4). Cave passage length peaks at three elevations: around 1400 m a.s.l. (~200 m of passage length), between 1600 and 1700 m a.s.l. (~300 m of passage length) and there are more than 700 m of cave passage distributed between 2000 and 2300 m a.s.l. Caves and other karst features at the highest elevations typically comprise small rock arches and other cave ruins that have been heavily affected by erosion and weathering. Correlation of the elevation distribution of the length of cave passages fits, though not perfectly, with the elevation distribution of the area of planation surface: some 8 km^2 of planation surfaces were mapped at 1600 m elevation and almost 10 km^2 at around 2200 m (Fig. 4). The planation surface maxima at 1600 m a.s.l. is too low elevated for the Giant cave level at ~1700 m a.s.l., as phreatic caves form at or below the paleo-base level. We argue that the maxima got shifted downwards due to widespread slope movements in the WNT. All planation surfaces are also marked by abundant dolines and other surface karst features. These features are particularly concentrated at the 2200 m planation level (e.g. next to Akarscharte at Kalkspitze and Gasthofkar north of Mosermandl). No lithology or structural control of planation surfaces was observed. Fluvial pebbles of the Augenstein Formation were found as a few isolated pockets in small dolines and faults on shallow slopes at about 2200 m a.s.l. Augenstein deposits were also found in several small caves including Durchgangshöhle.

3.3.1. Durchgangshöhle

This cave (Austrian cave register no. 2622/2) is of particular interest, because it contains abundant quartz pebbles of the Augenstein Formation and is one of the highest known caves in the area. These pebbles are an important geomorphic marker, because their influx into the cave likely occurred as the cave was located at base level (Wagner et al., 2011). Most of the cave developed in limestones of the Bänderkalkmarmor on the southern ridge of Steirische Kalkspitze next to the trail between Steirische Kalkspitze and Lungauer Kalkspitze at an elevation of 2340 m (47.2814°N, 13.6228°E; Figs. 3a, b, 6a). The cave has a total length of 320 m and consists of a maze of narrow passages distributed over about 30 m vertical and <100 m horizontal extent (Fig. 6d). Its name is derived from the two entrances joined by a straight passage. Both entrances are heavily weathered by frost shattering and lack primary karst dissolution features. However, the inner passages preserve near-circular cross sections (usually 1–2 m in diameter) of phreatic origin, dissected by canyons (Fig. 6b). Crystalline fluvial pebbles of the Augenstein Formation are common in these passages, e.g. as conglomerate pockets or single grains on the cave walls. There, they are typically covered by calcite speleothems up to ~10 cm thick (Figs. 6c, 7a). Reworked quartz pebbles are also present in the canyons, sometimes together with fine grained sediment derived from clastic deposits in the higher phreatic passages. Individual pebbles are 1–10 cm in size, well rounded and mostly quartz, but quartzite, mica schist and gneiss pebbles were also found. Only a few pebbles are lithologically similar to the Lantschfeld quartzite that constitutes the summit of Kalkspitze.

4. Geochronology and isotope geochemistry

In order to constrain the depositional age of the fluvial deposits in Durchgangshöhle and ultimately place constraints on the surface uplift history of the WNT region, several methods were applied. Firstly, we present stable isotope and geochronological data for a flowstone (speleothem) overgrowing pebbles in Durchgangshöhle at 2340 m

Fig. 3. Field impressions of the study area. (a) Kalkspitzen massif viewed from SW, with the summits of Steirische Kalkspitze (left) and Lungauer Kalkspitze (right) and Akarscharte in between. Durchgangshöhle cave is marked by the red arrow. (b) Steirische Kalkspitze seen from Lungauer Kalkspitze. The upper and lower entrances of Durchgangshöhle are marked by the red arrows. (c) Panoramic view of the study area. The Dachstein massif with its paleosurface is on the right side and the Niedere and Hohe Tauern are on the left side of the picture in the foreground and background, respectively. The SEMP fault zone runs along the cloud-filled valley (source: www.alpengeologie.org). (d) Augenstein deposit where sample KRM was collected, covered by vegetation. Person for scale. (e) Augenstein deposit preserved in a fault near Durchgangshöhle. (f) Augenstein deposit at the upper entrance of Durchgangshöhle. Carabiner for scale. (g) Planation surfaces in the WNT region as seen from Glocknerin to the east. The three mapped planation surfaces are shown by colored overlays. (h) Augenstein deposit at Niederer Gjaidstein on the Dachstein paleosurface. The quartz pebble is ~15 cm long. (i) Augenstein deposit at Hochkönig in the NCA. Pencil for scale. (j) Augenstein deposit at Streitmandlscharte in the NCA. Pebbles are 2–3 cm in diameter.

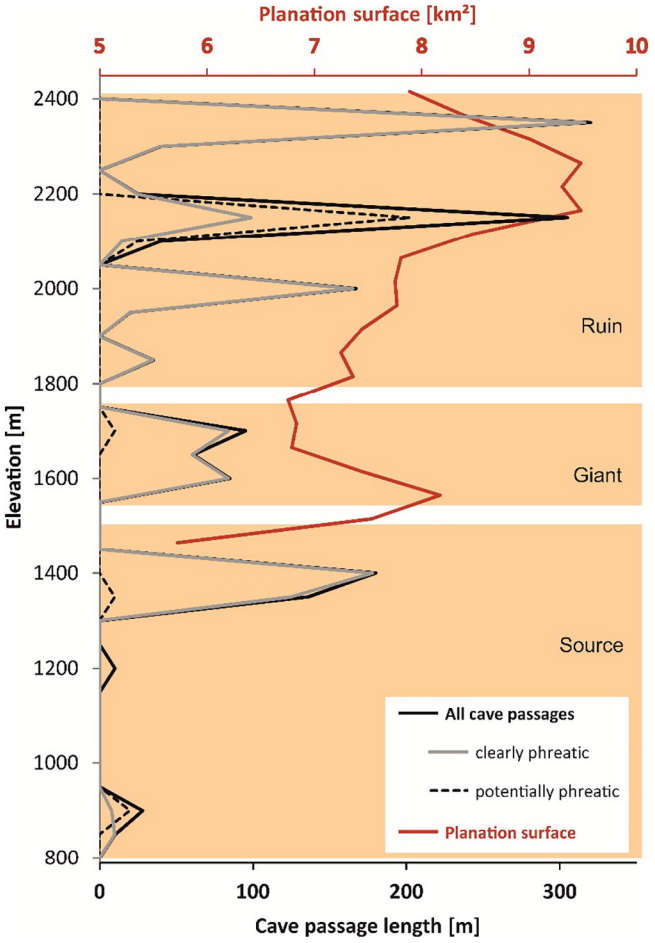

Fig. 4. Total length of cave passages as a function of elevation (in 50 m steps) and in comparison to the areas of planation surfaces for the western Niedere Tauern (WNT). The shaded regions for Ruin, Giant and Source are the elevation ranges for these three main cave levels in the NCA. For cave locations and planation surface distribution see Figs. 2a and b.

a.s.l. (Figs. 6c, 7a). Secondly, we report cosmogenic ^{21}Ne exposure history data of Augenstein quartz pebbles collected at several surface locations in the NCA and the WNT region (Fig. 1).

4.1. Samples and analytical techniques

The flowstone from the Durchgangshöhle consists of a 5 cm-thick calcite crust on top of crystalline gravel which was found as a pocket of calcite-cemented Augenstein pebbles on the cave wall (Figs. 6c, 7a). Its petrography was examined in thin sections using transmitted-light and epifluorescence microscopy. X-ray diffraction (XRD) was used to identify its mineralogy. Oxygen and carbon isotope compositions of the calcite were determined on samples hand-drilled across the speleothem crust. Results are expressed in per mil relative to the VPDB standard (Spötl and Vennemann, 2003). A preliminary geochronological analysis using the U-Th disequilibrium dating method yielded an age beyond the range of this technique, i.e. higher than ~500–600 ka. Therefore, the U-Pb dating method was applied in an attempt to determine the age of the calcite. To screen the sample a priori for trace element contents a 12-point profile was measured across the calcite crust using laser ablation ICP-MS (Fig. 7c).

The analytical method for U-Pb dating employed in this study followed closely those published previously by Woodhead et al. (2006, 2012). Multiple aliquots, typically weighing ~50 mg, were removed from a single growth layer of the flowstone. These calcite subsamples were then placed into pre-cleaned disposable polyethylene cups and moved to a multiple HEPA-filtered clean room environment. Samples were briefly leached twice in very dilute (~0.01 M) 3× teflon-distilled HCl, with each cycle lasting around 1 min, and then repeatedly washed in ultra-pure water before being dried in a HEPA-filtered laminar flow hood. This step is critical to the elimination of Pb contaminants resulting from sample handling which can easily dominate the Pb budget of the entire sample unless removed.

Individual samples were weighed into pre-cleaned Teflon beakers and treated with sufficient 6 N HCl to ensure complete dissolution. A mixed ^{233}U-^{205}Pb tracer, calibrated against EarthTime (http://www.earth-time.org) reference solutions, was then weighed into the vials and each one sealed and refluxed on the hotplate for several hours to ensure complete sample-spike equilibration. Samples were then dried down and taken up in 0.6 N HBr for Pb separation using AG 1X-8 anion exchange resin. The eluate was subsequently processed through the same column now filled with Eichrom TRU ion-specific resin, to separate U.

Isotope ratios were determined on a Nu Plasma MC-ICPMS using a DSN-100 desolvation unit and MicroMist glass nebulizer, operating in the range 50–100 μl/min uptake. Instrumental mass bias effects were monitored and corrected using NIST SRM 981 reference material in the case of Pb, and the sample's internal ^{238}U/^{235}U ratio in the case of U. Instrument data files were processed initially using an in-house designed importer, operating within the Iolite environment (Paton et al., 2011), which considers all data and reference material analyses obtained throughout a particular analytical session and permits a variety of corrections for instrumental mass bias and drift. The resulting data, now corrected for instrumental effects, were then blank corrected and isotope-dilution calculations performed using the software of Schmitz and Schoene (2007).

Cosmogenic ^{21}Ne was determined in quartz pebbles from the Augenstein Formation found at or near the surface. These relict sediments occur on many paleosurfaces in the NCA and the WNT (Fig. 1) at variable depth within the soil or sediment, but are rarely found exposed on the surface (Table 1). Sample VB was collected at an elevation of 1440 m a.s.l. ~3 m below the surface on Viehbergalm in the NCA on a paleosurfaces that smoothly passes into the Dachstein paleosurface at above 1800 m a.s.l. The location features a 5 to 8 m-thick Augenstein deposit cut by a creek. The Viehbergalm sample was therefore probably not exposed to cosmic radiation since its deposition in the Oligocene. It thus provides an estimate of the nucleogenic Ne accumulated since rock crystallization and the amount of cosmogenic Ne acquired during sediment transport in Oligocene. Samples KRM and GJ IV were collected on the Dachstein plateau itself (Fig. 1). The area corresponds to the oldest and highest planation surface in the NCA that also bears the Ruin cave level. It also represents the type locality of the Augenstein Formation, the so-called Augensteindlgrube at an elevation of 1800 m a.s.l. (47.508°N, 13.676°E) (Frisch et al., 2002), about 3 km northwest of sample location GJ IV. Sample GJ IV was a surface sample obtained from a pre-Pleistocene river channel near the flat summit of Niederer Gjaidstein (Fig. 3h). Sample KRM was collected in the northern part of the Dachstein plateau ~5 cm below the surface in a gravel-filled shallow doline (Fig. 3d). Sample ADA I was collected near Androthalm at an elevation of 1546 m a.s.l. on Hochschwab, eastern NCA (Fig. 1). The pebbles were buried by ~30 cm of soil at the rim of a vegetated doline. The area corresponds to the Dachstein paleosurface at Hochschwab. Sample SMS II was collected in a limestone fissure at an elevation of 2268 m a.s.l. near Streitmandlscharte on Tennengebirge (central NCA). The area corresponds to the Dachstein paleosurface and the Ruin cave level. Sample WS I was obtained from the northern side of the Enns valley near Wörschach at an elevation of 744 m a.s.l. buried beneath ~10 cm of sediment. These pebbles are part of the Miocene basin fill of this valley, which has been interpreted as a mixture of crystalline Austroalpine sediment derived from the Niedere Tauern and minor contributions of reworked Augenstein sediments (Keil and Neubauer, 2011a). Sample

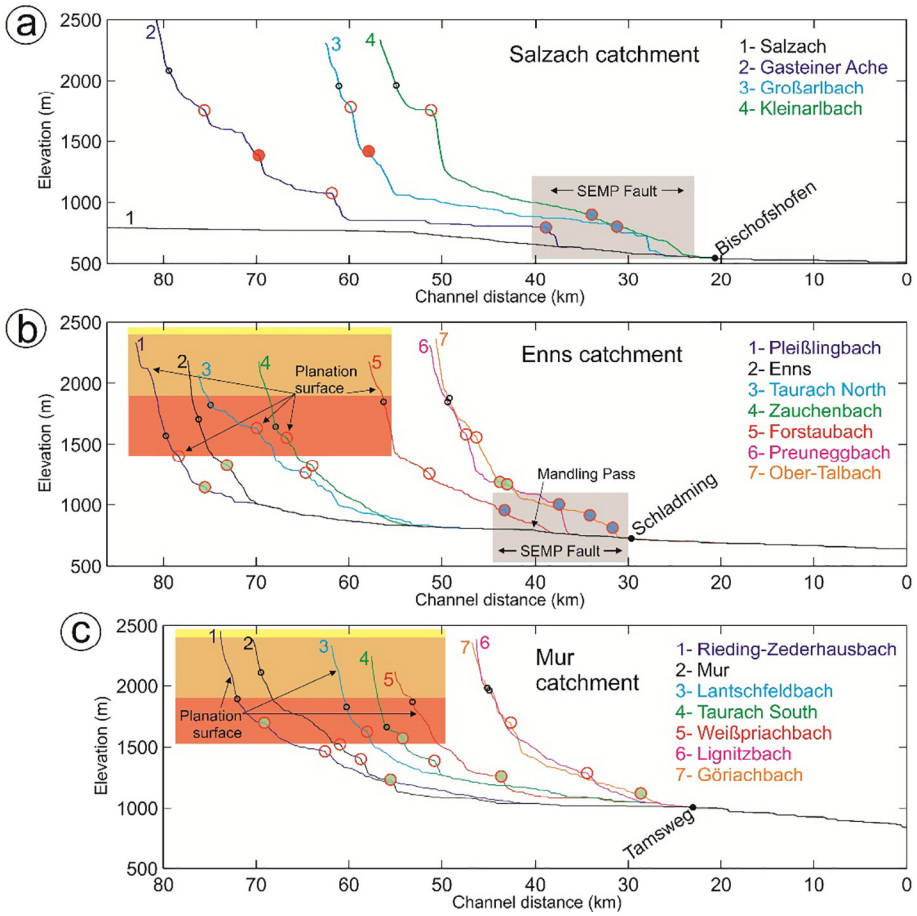

Fig. 5. Channel profiles of selected rivers in the Niedere Tauern region. The color coding and symbols correspond to those in Fig. 2b. Yellow, beige and brown areas indicate planation surfaces. The rivers run into the base levels of (a) Salzach, (b) Enns and (c) Mur.

KSP II is the only one from the WNT, collected ~5 cm below the surface next to the upper entrance of Durchgangshöhle at an elevation of 2370 m a.s.l. (Figs. 3f, 6a), which is part of the highest planation surface of the WNT. Further localities (Figs. 3i, j) were sampled and analyzed, but ^{21}Ne dating was unfruitful.

The quartz pebbles were crushed and the 50–100 μm grain size fraction was separated. Mineral impurities were removed by hand-picking under a binocular microscope, and the samples were then subjected to a HF-HNO_3 acid leach, followed by washes in de-ionized water and acetone. Approximately 200 mg of each sample were wrapped in Al foil. The samples were heated to 1200 °C in an ultra-high vacuum furnace, and the Ne isotope composition was determined using procedures reported in Codillean et al. (2008). The cosmogenic Ne production rate for each sample was scaled using the sea level high latitude (SLHL) rate and the Lal-Stone algorithm (Stone, 2000). The SLHL production rate of 15.7 atoms/g/year has been determined from the latest SLHL production rate scaling of ^{10}Be (Phillips et al., 2016).

4.2. Flowstone petrography, composition and age

The flowstone from Durchgangshöhle is composed of a translucent elongate-columnar fabric separated by a few thin layers which appear dark in transmitted light and white in reflected light. The latter layers are composed of micrite (Fig. 7b). Near the base a thin and discontinuous layer is present which consists of radiating crystals which reveal relict fibrous subcrystals, resembling aragonite. XRD analyses showed that all layers consist of low-Mg calcite. The thick elongate-columnar layers and the fibrous crystals revealed no fluorescence, while the thin whitish layers show moderately bright epifluorescence.

4.2.1. Stable isotopes and trace elements

δ^{13}C and δ^{18}O values of the flowstone range from +0.9 to +10.0‰ and from −10.9 to −6.7‰, respectively (Fig. 8). Samples of the hostrock limestone show a similar range in δ^{18}O and a narrower range in δ^{13}C values (+1.6 to +4.3‰). Laser ablation ICP-MS analyses of the flowstone (Fig. 7c) yielded variable concentrations of Mg (7151–11,776 ppm, mean 8480 ppm), Sr (138–517 ppm, mean 255 ppm), Ba (8–30 ppm, mean 16 ppm) and U (0.9–20.3, mean 7.6 ppm). Pb values range from below detection (0.004–0.005 ppm) to 0.35 ppm (mean 0.1 ppm).

4.2.2. U-Pb dating

In order to facilitate the choice of layers to sample for U-Pb dating a second laser ablation ICP-MS profile was acquired measuring U and Pb concentrations. The zone with the highest U/Pb ratios (Fig. 9), which is composed of elongate-columnar calcite, was then sub-sampled using a dental drill. Although Pb contents extend up to 0.3 ppm, suggesting some initial 'common Pb' component, U concentrations were typically high (1–18 ppm; corresponds to sampled aliquots) allowing a relatively precise age determination. Isochron ages were determined using in-house software, assuming negligible initial ^{230}Th and ^{234}U/^{238}U ratios measured previously. Using the measured ^{234}U/^{238}U ratio of 0.9896 ± 0.0017 to provide a robust correction for initial disequilibrium in the U-series decay chain resulted in a disequilibrium-corrected U-Pb age of 682 ± 17 ka (Table 2).

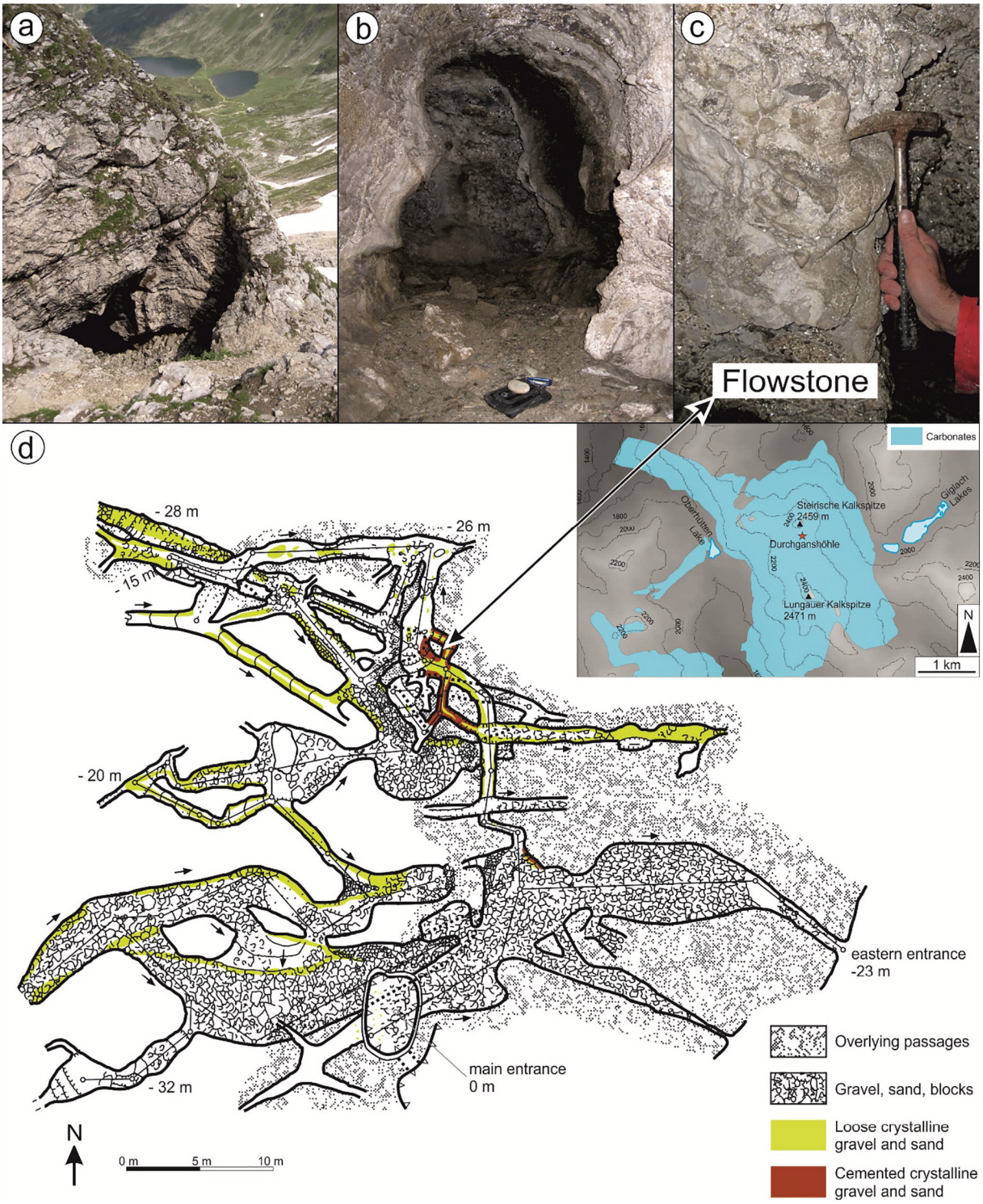

Fig. 6. Pictures and cave map of Durchgangshöhle. (a) Upper entrance of the cave next to the path leading to the summit of Steirische Kalkspitze. The doline is ~3 m deep. Giglach lakes in the background. (b) A paleo-phreatic section of the cave with crystalline fluvial gravel cemented onto the walls and loose pebbles on the ground. Pocket camera bag for scale. (c) Flowstone on top of gravel on cave wall. (d) Plan view of Durchgangshöhle (by E. Dachs, 1978 in Klappacher, 1992). Occurrence of Augenstein pebbles mapped in this study are shown in yellow and brown.

4.3. Cosmogenic Ne exposure ages

All analyzed samples plot within their two sigma errors on the air-cosmogenic Ne mixing line (not shown), which is consistent with Ne being derived from these two sources. However, Ne derived from nucleogenic processes in the crust is isotopically similar to cosmogenic Ne, and the analytical uncertainties may obscure the presence of a small contribution of nucleogenic ^{21}Ne generated since the time of quartz crystallization (Niedermann, 2002). We used the non-atmospheric ^{21}Ne in recently exposed quartz pebbles from the shielded gravel deposit at Viehbergalm (VB) to quantify the contribution of nucleogenic ^{21}Ne and cosmogenic ^{21}Ne generated during erosion and

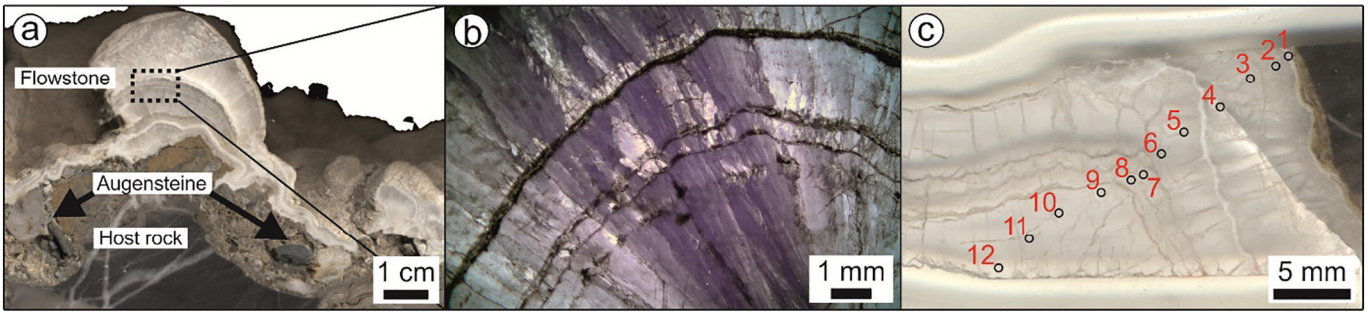

Fig. 7. Flowstone specimen from Durchgangshöhle: (a) Overview of cut sample with the main flowstone (this sample does not correspond exactly to Figs. 7c, 8 (data points) and 9, but all samples are within a few centimeters of each other). (b) Thin section image (transmitted light, partially crossed nicols) showing translucent columnar calcite crystals and thin micritic layers. (c) Sampling spots for geochemical data. Data in Supplementary Table S1.

transport from the source area in the south, during the Oligocene. The ^{21}Ne concentration of this sample ($5.9 \pm 3.2 \times 10^6$ atoms/g) is higher than that measured in higher elevation surface samples buried at shallow depth, e.g. SMS I, KRM and KSP II. This suggests that this value is a good estimate of the concentration of ^{21}Ne generated in pebbles prior to exposure since the removal of the Augenstein cover during the Pleistocene glaciations. Two pebbles from the Dachstein paleosurface (GJ IV and ADA I) yielded ^{21}Ne concentrations significantly higher than the background level. The excess ^{21}Ne (1.5×10^7 atoms/g) is equivalent to minimum exposure durations of 115 and 262 ka. As these pebbles have been eroded from the gravel, the cosmogenic ^{21}Ne data reflect the minimum time these pebbles have been at or near the Earth's surface.

5. Discussion

The mapped surface features allow some indirect constraints to be placed on the landscape and climate evolution of the WNT region and ultimately on the Eastern Alps as a whole. The Pleistocene U-Pb age of the flowstone and the inferred ^{21}Ne ages of the surface Augenstein deposits represent a younger stage of the landscape evolution. Regrettably, they do not reflect aspects of the earlier deposition history of these sediments but help to constrain the glacial history.

Cave levels and planation surfaces in the Niedere Tauern (Fig. 4) correlate with those in the NCA (Fig. 10) if we consider highest uplift rates in the Tauern Window (Fig. 1) (Hofmann and Schönlaub, 2007). The three levels described here for the WNT at 2300 m, 1700 m and 1400 m a.s.l. correspond to the Ruin, Giant and Source level in the NCA (Fischer, 1990; Wisshak and Jantschke, 2010). The corresponding three levels in the NCA vary somewhat in elevation between different subregions within the NCA. For example, the Steinernes Meer region shows cave level maxima similar to those of the WNT at approximately 2400 m, 2200 m and 1000 m a.s.l. Although Ruin and Giant levels are higher, the Source level maximum is a few hundred meters lower in comparison to the WNT. In the Tennengebirge massif, the Ruin (2000 m) and Source levels (1000 m) are somewhat lower than in the WNT, but the Giant level is at exactly the same elevation (1700 m). Ruin, Giant and Source levels in the Untersberg massif and the western Totes Gebirge region are located at 1700 m, 1500–1400 m and 700 m a.s.l., respectively. In summary, the high degree of correlation of cave levels and planation surfaces between the WNT and the NCA implies that the vertical displacement along the SEMP since the Miocene is small, which is partly in contrast to the interpretation of Keil and Neubauer (2011a).

Distinct knickpoints of the south-north and north-south flowing streams that drain the WNT region to the Salzach/Enns and Mur valleys, respectively, can also be correlated with the lower planation surface at 1600 m a.s.l. as mapped here (Figs. 2b, 5b, c). Though the intermediate planation surface at ~2200 m a.s.l. is evident in some channel profiles, no clear evidence of knickpoints was found, as this region lies almost completely above the critical catchment area of 1 km^2 where fluvial erosion laws fail. One knickpoint of the Gasteinerache and the Großarlbach correlates with a lithology change from the Subpenninic gneiss cores to the Penninic schistose rocks in the Tauern Window. A number of streams contain also low-level knickpoints that relate to base-level lowering during the glaciation periods. (Figs. 5a, b). This interpretation of the lowest knickpoints is supported by the difference between the streams draining into the Salzach and into the Enns: the three analyzed streams draining to the Salzach have substantial knickpoints of 100–200 m above their confluence with the Salzach. The Salzach itself established its course between Zell am See and Bischofshofen not before the Pleistocene glaciations causing a base-level lowering of some 100–200 m (Robl et al., 2008). The easternmost Kleinarlbach shows no elevation step for the lowermost knickpoint converging the SEMP fault, due to mass movements within soft black slates of the Greywacke Zone. Knickpoints of the streams draining into the Enns also correlate with mass movements (Figs. 2b, 5b). Only the Forstau-, Preunegg- and the Ober-Talbach near Schladming show knickpoints at the confluence with the Enns (converging the SEMP Fault). In contrast to the streams draining into the uppermost Enns, these three streams drain the Enns downstream of the Mandling Pass (Figs. 2b, 5b). This suggests that the Mandling Pass played a role in base-level lowering

Table 1
Coordinates of the sampled Augenstein pebbles and ^{21}Ne data of analyzed quartz pebbles. Minimal exposure ages are given for samples GJ IV and ADA I with excess ^{21}Ne.

Sample	Location	Long. [°]	Lat. [°]	Elevation [m a.s.l.]	^{21}Ne[a] [10^6 a/g]	^{21}Ne$_{cos}$[b] [10^6 a/g]	P ^{21}Ne[c] [a/g/yr]	Minimum exposure age [yr]
VB	Viehbergalm	13.847	47.495	1440	5.9 ± 3.2			
KRM	Krippenstein Margschief	13.713	47.516	1984	3.2 ± 2.0			
KSP II	Kalkspitze	13.623	47.281	2370	5.7 ± 1.6			
GJ IV	Gjaidstein	13.645	47.487	2475	20 ± 3.4	14 ± 3.4	130	114,500
ADA I	Androthalm	15.001	47.587	1546	22 ± 4.4	16 ± 4.4	65	261,500
SMS II	Streitmandl-scharte	13.245	47.507	2268	4.5 ± 2.1			
WS I	Wörschach-Fürstensteig	14.131	47.549	744	1.0 ± 1.1			

[a] Concentration of ^{21}Ne in excess of that derived from air.
[b] Concentration of cosmogenic ^{21}Ne corrected for nucleogenic and pre-exposure ^{21}Ne.
[c] Sample specific cosmogenic ^{21}Ne production rate.

due to glacial overdeeping downstream (Keil and Neubauer, 2011b). Rivers draining southward into the Mur show similar characteristics to the upper Enns drainages and some have pronounced knickpoints near their confluence with the Mur. Other knickpoints can also mostly be related to mass movements as shown on Figs. 2b and 5.

The U-Pb age of the flowstone (682 ± 17 ka) indicates a period of speleothem growth in Durchgangshöhle during the early part of the Middle Pleistocene. This age falls at the transition between Marine Isotope Stage (MIS) 17 and the following MIS 16 (based on the deep-sea stack of Lisiecki and Raymo, 2005). Taking the full error range into consideration, the calcite could have formed during the peak of the MIS 17 interglacial (696 ka) or during the first half the MIS 16 glacial. Slow modern surface uplift rates of the Kalkspitze region (~0.4 mm/a – Hofmann and Schönlaub, 2007) suggest a similar or slightly lower (by a few hundred meters) altitude of the cave some 680 ka ago. The topography was likely different from today as large subsequent glaciations shaped the alpine landscape.

The high degree of purity of the speleothem is consistent with other (younger) speleothems from high-altitude caves in the Alps and contrasts to the commonly less pure (and often brown-colored) samples from lower-elevation cave sites (Spötl et al., 2007). This degree of purity suggests little soil in the former catchment of the cave dripwater. The high to very high C isotope values (Fig. 8) also strongly suggest little or even no soil above the cave, although these data are clearly influenced by kinetic isotope fractionation similar to what has been observed in other high-alpine speleothems (e.g., Spötl and Mangini, 2007). The O isotope data show a spread of 4.2‰ (Fig. 8). Although these data may also have been affected by kinetic isotope fractionation to a small extent, they are broadly consistent with data from Holocene speleothems from caves, whose catchments are located at about 1900–2500 m, i.e. at a similar altitude as Durchgangshöhle, in other parts of the Eastern Alps (Mangini et al., 2005; Meyer et al., 2008; C. Spötl, unpublished data). These $\delta^{18}O$ values argue against a cold, glacial-type climate, as has been recorded by younger speleothems of highly depleted O isotope signature from high-alpine caves (Spötl and Mangini, 2007; Luetscher et al., 2015). Taken together, the currently available data suggest deposition of these speleothems during a climate period not drastically different from today.

The cosmogenic ^{21}Ne data of pebbles GJ IV (Dachstein) and ADA I (Hochschwab) place constraints on the erosion and exposure history of the Augenstein deposits. The data are interpreted in terms of a minimum cumulative total exposure time since their erosion from the Augenstein gravel of 115 and 262 ka, respectively. The pebbles have likely experienced several erosion cycles with different durations accumulating cosmogenic Ne while in the upper few meters below the surface. Most likely, all pebbles where initially buried underneath Augenstein cover at some time during the Oligocene, following an initial cycle of erosion, transportation and sedimentation. The Pleistocene glacial cycles likely involved major recycling and large amounts of the remaining Augenstein deposits on the NCA paleosurfaces were eroded. While the data confirm that the Augenstein pebbles have existed close to the erosional surface for several 100 ka, the exposure durations of both samples are significantly lower than expected if they had received cosmic radiation since the Oligocene. Most likely, these pebbles were buried underneath a thick Augenstein cover for most of the time since the Oligocene, until glacial cycles exposed them in the Pleistocene. Just two samples show ^{21}Ne data in excess which is striking, because samples KRM, KSP II and SMS II where even higher elevated, more shallow buried and show lower Ne values than sample VB. It should be taken into account that a variability of nucleogenic Ne might be present in the samples as the Augenstein quartz pebbles are composed of different lithologies.

Sample GJ IV from the flat summit plateau of Niederer Gjaidstein at the Dachstein massif yielded a shorter exposure duration of 115 ka. The Augenstein cover was likely thicker in the central NCA (Frisch et al., 2001) and further the glaciations had been more extensive in this region compared to the Hochschwab located to the east of the Alpine ice-stream network (Fig. 1). Both observations argue for a higher amount of shielding from cosmic radiation, due to a deeper burial of the pebbles and a longer glacial duration in the Dachstein region. The longer

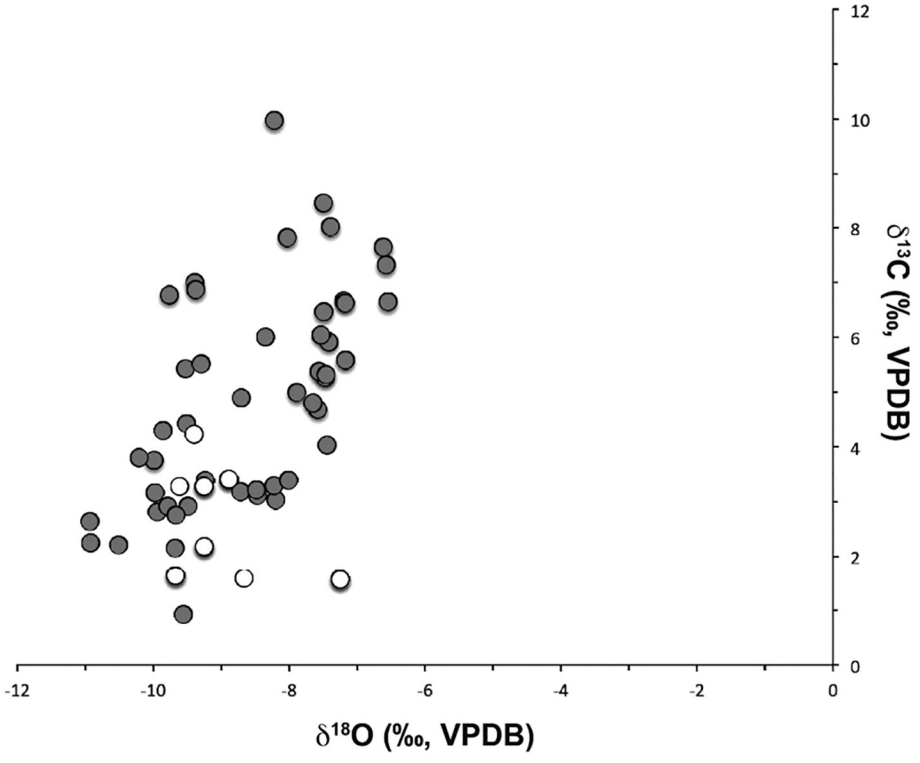

Fig. 8. Stable isotope composition of flowstone (grey symbols) compared to the hostrock (open symbols) from Durchgangshöhle. Data in Supplementary Table S2.

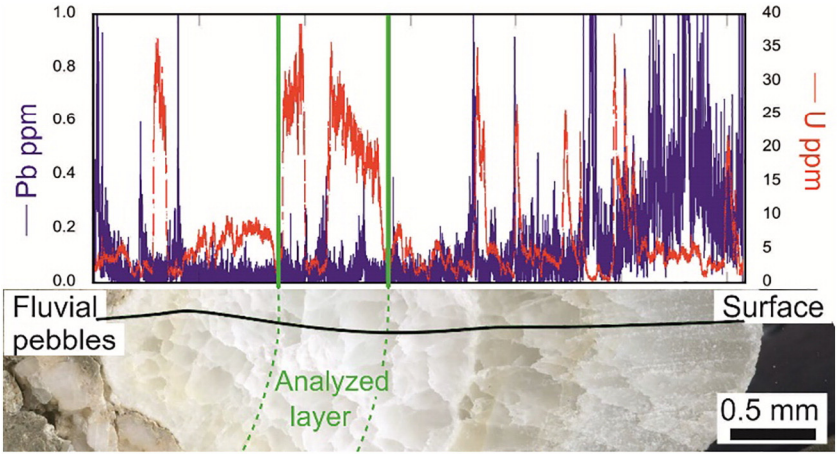

Fig. 9. Laser ablation ICP-MS profile across the flowstone. The green area was subsequently sampled for U-Pb dating (Table 2).

exposure duration of 262 ka of the Hochschwab sample is consistent with the longer transport distance from the source area (near the Tauern Window) and a thinner Augenstein cover in the eastern NCA.

5.1. Implications for the landscape evolution

The observations discussed above allow to place constraints on the landscape evolution of the WNT region since the Oligocene. The presence of fluvial gravels of the Augenstein formation at elevations of up to 2340 m a.s.l. on an isolated limestone peak clearly shows that the present-day topography is vastly different from that in the Oligocene. At that time, Durchgangshöhle formed in a subtropical climate (Kuhlemann et al., 2008) under phreatic conditions at the fluvial base level (Fig. 10). Somewhat later in the early Neogene, Augenstein gravel was fluvially transported to the study area from a southerly source and buried this karst landscape (Frisch et al., 2002; Keil and Neubauer, 2015). Subsequent surface uplift between 23 and 5 Ma is inferred from low-temperature geochronological data (Reinecker, 2000; Wölfler et al., 2012). The planation surfaces mapped here indicate that this uplift occurred in several steps. Surface uplift commenced somewhat earlier in the WNT than in the NCA resulting in a topographic south-north gradient. Formation of the Enns valley started around 18 Ma related to the SEMP (Ratschbacher et al., 1989; Keil and Neubauer, 2009) and the associated base-level lowering may relate to the discrete interruptions of the surface uplift indicated by the planation surfaces.

The fluvial deposits in Durchgangshöhle are interpreted to have been largely removed during base-level lowering and the initial relief formation of the Kalkspitze summit, most probably occurred at or soon after 18 Ma, related to early movements along the SEMP and the concomitant formation of the Enns valley. The lower Giant cave level also probably formed at that time, connected to base-level lowering in the Enns valley, subtropical climate conditions and abundant water supply. Canyons in Durchgangshöhle were cut under vadose conditions at this time. Surface uplift continued until the Kalkspitze region was covered by ice during the Pleistocene glaciations. Speleothems in Durchgangshöhle formed during MIS 17 or, less likely, during the first half of the following glacial period cementing remnants of the pebble deposits that had been largely removed by earlier erosional events. Erosion and frost shattering have partly exhumed and destroyed the cave and its entrances since then.

This landscape evolution model implies that the planation surfaces existed in both the NCA and the WNT well before the Pleistocene. Because of their karst origin and sediment cover they are clearly unrelated to what is known as the "glacial buzz saw" process (Sternai et al., 2012). This model has been held responsible for the fact that the topography becomes shallower at higher elevations in most parts of the Alps (Kühni and Pfiffner, 2001; Hergarten et al., 2010). Our data therefore demonstrate the partial preservation of geomorphic elements of the Miocene landscape despite the pervasive impact of the Pleistocene glaciations. Other models about the presence of shallow slopes at high elevations, in particular the model of fluvial immaturity of Hergarten et al. (2010), are therefore favored.

Table 2
U-Pb dating results.

Aliquot	$^{238}U/^{206}Pb$	2 sigma [%]	$^{207}Pb/^{206}Pb$	2 sigma [%]	Error correlat.
1	9247.64	1.04	0.2053	3.50	−0.9864
2	4530.88	0.58	0.5005	0.42	−0.8751
3	2150.94	0.85	0.6506	0.35	−0.9833
4	10,866.22	1.81	0.1219	11.67	−0.9977
5	9851.51	2.60	0.1445	13.77	−0.9989
6	2350.31	0.30	0.6460	0.14	−0.7836

6. Conclusions

The Kalkspitze region of the Niedere Tauern region is one of the few areas along the main divide of the Eastern Alps that consists of karstified limestones. The region is therefore well suited to study the landscape evolution of the mountain range and to compare it to the surface uplift history of the Northern Calcareous Alps to the North. Both regions share features including planation surfaces, karst caves and fluvial gravels of the Augenstein deposits.

Cave levels and planation surfaces in the Niedere Tauern are located at three distinct elevations (2000–2400 m, 1600–1700 m and 1400 m) and that correlate with the Ruin, Giant and Source levels in the Northern Calcareous Alps. The good correlation with the levels in the NCA suggests negligible vertical movements along the major fault zone (SEMP) that has separated the WNT from the NCA since the Miocene.

Planation surfaces in the Niedere Tauern are generally karstified suggesting that these surfaces date back to the Neogene. In essence, our observations support a preservation of Neogene landforms despite of intensive glacial erosion during the Pleistocene.

U-Pb dating of flowstone capping fluvial pebbles in Durchgangshöhle yielded an age of 682 ± 17 ka indicating conditions favorable for karstification and speleothem deposition during the MIS 17 interglacial or the transition into the following cold period. C and O isotope data of the flowstone, although compromised by kinetic fractionation, suggest temperatures broadly similar to today and little or almost no vegetation and soil above the former catchment of the cave.

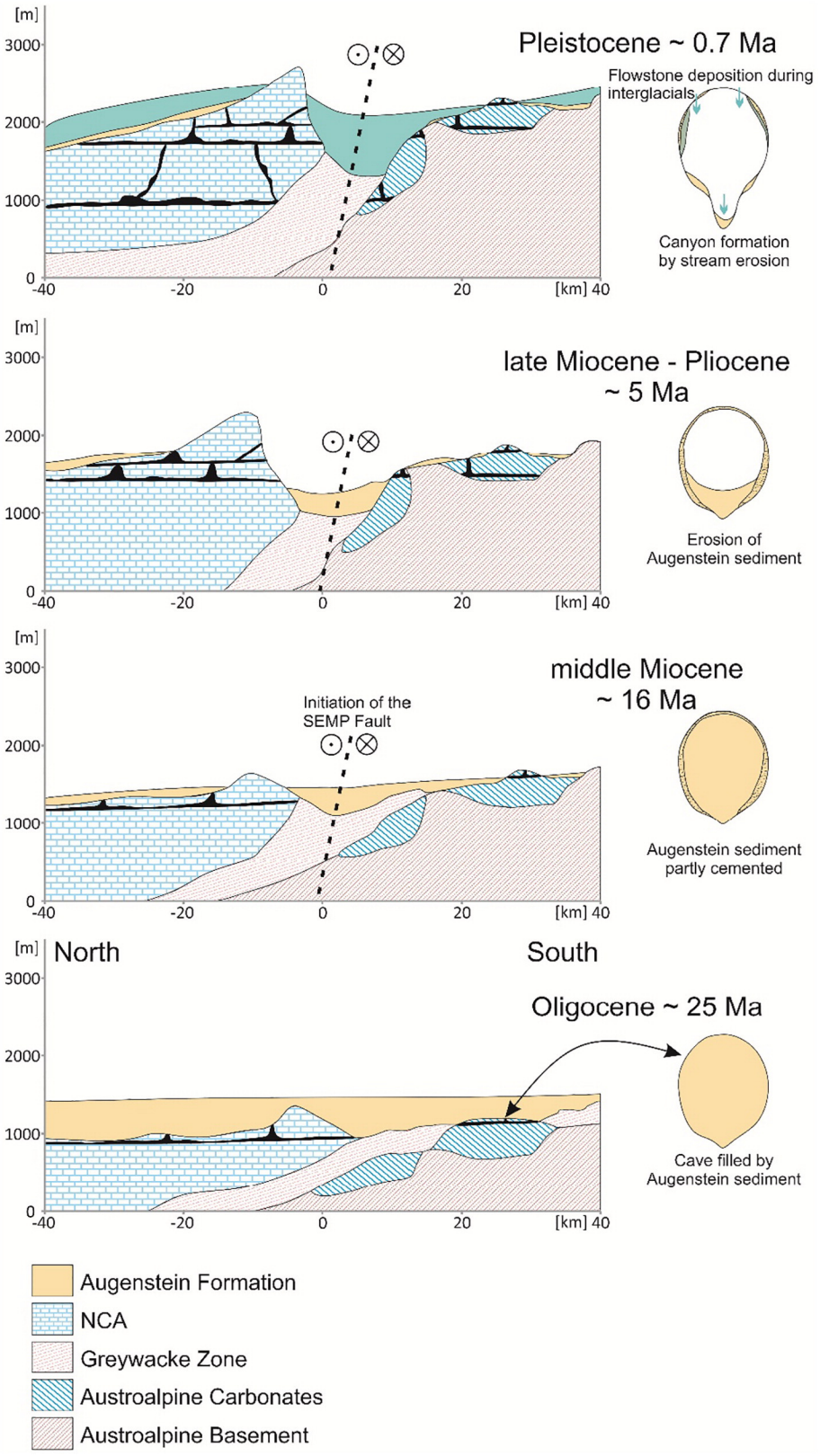

Fig. 10. Sketch of the landscape evolution of the Niedere Tauern and the Dachstein Plateau since the Oligocene. The evolution of the Durchgangshöhle is schematically shown on the right side.

^{21}Ne analyses of two Augenstein pebbles from the NCA (Gjaidstein on Dachstein paleosurface and from Hochschwab) yielded ages of 115 and 262 ka. We attribute the younger age (from Gjaidstein) to the (initially) thicker Augenstein cover on the Dachstein and the longer time span during which this sample was shielded from cosmic radiation by a glacier. The Hochschwab sample underwent a longer transport history and was likely buried beneath a thinner Augenstein cover.

Acknowledgements

C. Weiss, S. Hofer, A. Klarström and H. Kovac helped in the field. R. Boch, G. Bryda, E. Dachs, E. Herrmann, G. Höfer-Öllinger, G. Mandl and the Salzburger Höhlenverein are thanked for discussing Augenstein locations and further information concerning the Niedere Tauern area. Luigia DiNicola is thanked for her effort in the cosmogenic Ne laboratory. Ph. Häuselmann, M. Stokes and an anonymous reviewer are thanked for their constructive comments.

Appendix A. Supplementary data

Supplementary data to this article can be found online at https://doi.org/10.1016/j.geomorph.2017.09.024.

References

Bartosch, T., Stüwe, K., Robl, J., 2017. Topographic evolution of the Eastern Alps: the influence of strike-slip faulting activity. Lithosphere 9:384–398. https://doi.org/10.1130/L594.1.

Braunstingl, R., Pestal, G., Hejl, E., Egger, H., van Husen, D., Linner, M., Mandl, G., Moser, M., Reitner, J., Rupp, C., Schuster, R., 2005. Geologische Karte von Salzburg 1:200.000. Geologische Bundesanstalt, Vienna.

Champagnac, J.D., Schlunegger, F., Norton, K., von Blanckenburg, F., Abbühl, L.M., Schwab, M., 2009. Erosion-driven uplift of the modern Central Alps. Tectonophysics 474: 236–249. https://doi.org/10.1016/j.tecto.2009.02.024.

Codillean, A., Bishop, P., Stuart, F., Hoey, T., Fabel, D., Freeman, S., 2008. Single-grain cosmogenic ^{21}Ne concentrations in fluvial sediments reveal spatially variable erosion rates. Geology 36:159–162. https://doi.org/10.1130/G24360A.1.

Decker, K., Peresson, H., 1996. Tertiary kinematics in the Alpine-Carpathian-Pannonian system: links between thrusting, transform faulting and crustal extension. In: Wessely, G., Liebl, W. (Eds.), Oil and Gas in Alpine Thrustbelts and Basins of Central and Eastern Europe, EAGE Special Publications. 5, pp. 69–77.

Fischer, K., 1990. Höhlenniveaus und Altreliefgenerationen in den Berchtesgadener Alpen. Mitteilungen der Geographischen Gesellschaft in München 75, 47–59.

Frisch, W., 1979. Tectonic progradation and plate tectonic evolution of the Alps. Tectonophysics 60:121–139. https://doi.org/10.1016/0040-1951(79)90155-0.

Frisch, W., Kuhlemann, J., Dunkl, I., Brügel, A., 1998. Palinspastic reconstruction and topographic evolution of the eastern Alps during the Late Tertiary extrusion. Tectonophysics 297:1–15. https://doi.org/10.1016/S0040-1951(98)00160-7.

Frisch, W., Kuhlemann, J., Dunkl, I., Székely, B., 2001. The Dachstein paleosurface and the Augenstein Formation in the Northern Calcareous Alps — a mosaic stone in the geomorphological evolution of the Eastern Alps. Int. J. Earth Sci. 90:500–518. https://doi.org/10.1007/s005310000189.

Frisch, W., Kuhlemann, J., Dunkl, I., Székely, B., Vennemann, T., Rettenbacher, A., 2002. Dachstein-Altfläche, Augenstein-Formation und Höhlenentwicklung — die Geschichte der letzten 35 Millionen Jahre in den zentralen Nördlichen Kalkalpen. Die Höhle 53:1–36. http://www.zobodat.at/pdf/Hoehle_053_0001-0035.pdf.

Genser, J., van Wees, J.D., Cloetingh, S., Neubauer, F., 1996. Eastern Alpine tectono-metamorphic evolution –constraints from 2-dimensional P-T-t modeling. Tectonics 15:584–604. https://doi.org/10.1029/95TC03289.

Harmand, D., Adamson, K., Rixhon, G., Jaillet, S., Losson, B., Devos, A., Hez, G., Calvet, M., Audra, P., 2017. Relationships between fluvial evolution and karstification related to climatic, tectonic and eustatic forcing in temperate regions. Quat. Sci. Rev. 166: 38–56. https://doi.org/10.1016/j.quascirev.2017.02.016.

Hejl, E., 1997. 'Cold spots' during the Cenozoic evolution of the Eastern Alps: thermochronological interpretation of apatite fission-track data. Tectonophysics 272:159–173. https://doi.org/10.1016/S0040-1951(96)00256-9.

Herbst, J., 1985. Die Ur–Salzach–Schüttung. Doctoral Thesis. University of Salzburg, Salzburg, Austria 138pp.

Hergarten, S., Wagner, T., Stüwe, K., 2010. Age and prematurity of the Alps derived from topography. Earth Planet. Sci. Lett. 297:453–460. https://doi.org/10.1016/j.epsl.2010.06.048.

Hofmann, T., Schönlaub, H.P., 2007. Geo-Atlas Österreich. Vienna (Böhlau).

van Husen, D., 2000. Geological processes during the Quaternary. Mitteilungen der Österreichischen Geologischen Gesellschaft 92, 135–156.

Keil, M., Neubauer, F., 2009. Initiation and development of a fault-controlled, orogen-parallel overdeepened valley: the Upper Enns Valley, Austria. Austrian Journal of Earth Sciences 102:80–90. http://www.univie.ac.at/ajes/archive/volume_102_1/keil_neubauer_ajes_v102_1.pdf.

Keil, M., Neubauer, F., 2011a. The Miocene Enns Valley basin (Austria) and the North Enns Valley fault. Austrian Journal of Earth Sciences 104:49–65. http://www.univie.ac.at/ajes/archive/volume_104_1/keil_neubauer_ajes_v104_1.pdf.

Keil, M., Neubauer, F., 2011b. Neotectonics, drainage pattern and geomorphology of the orogen-parallel Upper Enns Valley, Eastern Alps. Geol. Carpath. 62:279–295. https://doi.org/10.2478/v10096-011-0022-y.

Keil, M., Neubauer, F., 2015. Orogen-parallel extension and topographic gradients east of the Tauern window: a possible indication of intra-orogenic raft tectonics? Austrian Journal of Earth Sciences 108:4–15. https://doi.org/10.17738/ajes.2015.0001.

Klappacher, W., 1992. Salzburger Höhlenbuch Band 5. Salzburger Mittelgebirge und Zentralalpen. Salzburg, Salzburg, Landesverein für Höhlenkunde in 625 pp.

Kuhlemann, J., 2007. Paleogeographic and paleotopographic evolution of the Swiss and Eastern Alps since the Oligocene. Glob. Planet. Chang. 58:224–236. https://doi.org/10.1016/j.gloplacha.2007.03.007.

Kuhlemann, J., Frisch, W., Szekely, B., Dunkl, I., Kazmer, M., 2002. Postcollisional sediment budget history of the Alps: tectonic versus climatic control. Int. J. Earth Sci. 91: 818–837. https://doi.org/10.1007/s00531-002-0266-y.

Kuhlemann, J., Taubald, H., Vennemann, T., Dunkl, I., Frisch, W., 2008. Clay mineral and geochemical composition of Cenozoic paleosol in the Eastern Alps (Austria). Austrian Journal of Earth Sciences 101:60–69. http://www.univie.ac.at/ajes/archive/volume_101/kuhlemann_et_al_ajes_v101.pdf.

Kühni, A., Pfiffner, O.A., 2001. The relief of the Swiss Alps and adjacent areas and its relation to lithology and structure: topographic analysis from a 250-m DEM. Geomorphology 41:285–307. https://doi.org/10.1016/S0169-555X(01)00060-5.

Legrain, N., Stüwe, K., Wölfler, A., 2014. Incised relict landscapes in the eastern Alps. Geomorphology 221:124–138. https://doi.org/10.1016/j.geomorph.2014.06.010.

Legrain, N., Dixon, J., Stüwe, K., von Blanckenburg, F., Kubik, P., 2015. Post-Miocene landscape rejuvenation at the eastern end of the Alps. Lithosphere 7:3–13. https://doi.org/10.1130/L391.1.

Linzer, H.F., Moser, F., Nemes, F., Ratschbacher, L., Sperner, B., 1997. Build-up and dismembering of the eastern Northern Calcareous Alps. Tectonophysics 272:97–124. https://doi.org/10.1016/S0040-1951(96)00254-5.

Lisiecki, L.E., Raymo, M.E., 2005. A Pliocene-Pleistocene stack of 57 globally distributed benthic δ^{18}O records. Paleoceanography 20, PA1003. https://doi.org/10.1029/2004PA001071.

Luetscher, M., Boch, R., Sodemann, H., Spötl, C., Cheng, H., Edwards, R.L., Frisia, S., Hof, F., Müller, W., 2015. North Atlantic storm track changes during the Last Glacial Maximum recorded by Alpine speleothems. Nat. Commun. 6:6344. https://doi.org/10.1038/ncomms7344.

Mangini, A., Spötl, C., Verdes, P., 2005. Reconstruction of temperature in the Central Alps during the past 2000 years from a δ^{18}O stalagmite record. Earth Planet. Sci. Lett. 235: 741–751. https://doi.org/10.1016/j.epsl.2005.05.010.

Meyer, M., Spötl, C., Mangini, A., 2008. The demise of the last interglacial recorded in -isotopically dated speleothems from the Alps. Quat. Sci. Rev. 27:476–496. https://doi.org/10.1016/j.quascirev.2007.11.005.

Montgomery, D.R., Korup, O., 2011. Preservation of inner gorges through repeated Alpine glaciations. Nat. Geosci. 4:62–67. https://doi.org/10.1038/ngeo1030.

Niedermann, S., 2002. Cosmic-ray-produced noble gases in terrestrial rocks: dating tools for surface processes. In: Porcelli, D., Ballentine, C., Wieler, R. (Eds.), Noble Gases in Geochemistry and Cosmochemistry. Reviews in Mineralogy and Geochemistry. 47:pp. 731–784. https://doi.org/10.2138/rmg.2002.47.16.

Palmer, A.N., 1987. Cave levels and their interpretations. NSS Bulletin 49:50–66. https://caves.org/pub/journal/NSS%20Bulletin/Vol%2049%20num%202.pdf.

Paton, C., Hellstrom, J., Paul, B., Woodhead, J., Hergt, J., 2011. Iolite: freeware for the visualisation and processing of mass spectrometer data. J. Anal. At. Spectrom. 26: 2508–2518. https://doi.org/10.1039/C1JA10172B.

Phillips, F.M., Argento, D.C., Balco, G., Caffee, M.W., Clem, J., Dunai, T.J., Finkel, R., Goehring, B., Gosse, J.C., Hudson, A.M., Jull, A.J.T., Kelly, M.A., Kurz, M., Lal, D., Lifton, N., Marrero, S.M., Nishiizumi, K., Reedy, R.C., Schäfer, J., Stone, J.O.H., Swanson, T., Zreda, M.G., 2016. The CRONUS-Earth Project: a synthesis. Quat. Geochronol. 31:119–154. https://doi.org/10.1016/j.quageo.2015.09.006.

Ratschbacher, L., 1986. Kinematics of Austro-Alpine cover nappes: changing translation path due to transpression. Tectonophysics 125:335–356. https://doi.org/10.1016/0040-1951(86)90170-8.

Ratschbacher, L., Frisch, W., Neubauer, F., Schmid, S.M., Neugebauer, J., 1989. Extension in compressional orogenic belts: the Eastern Alps. Geology 17:404–407. https://doi.org/10.1130/0091-7613(1989)017%3C0404:EICOBT%3E2.3.CO;2.

Ratschbacher, L., Frisch, W., Linzer, H.-G., Merle, O., 1991. Lateral extrusion in the Eastern Alps, part 2: structural analysis. Tectonics 10:257–271. https://doi.org/10.1029/90TC02623.

Reinecker, J., 2000. Stress and deformation: Miocene to present-day tectonics in the Eastern Alps. Tübinger Geowissenschaftliche Arbeiten Reihe A 55, 1–128.

Robl, J., Hergarten, S., Stüwe, K., 2008. Morphological analysis of the drainage system in the Eastern Alps. Tectonophysics 460:263–277. https://doi.org/10.1016/j.tecto.2008.08.024.

Schmid, S.M., Fügenschuh, B., Kissling, E., Schuster, R., 2004. Tectonic map and overall architecture of the Alpine orogen. Eclogae Geol. Helv. 97:93–117. https://doi.org/10.1007/s00015-004-1113-x.

Schmitz, M.D., Schoene, B., 2007. Derivation of Isotope Ratios, Errors, and Error Correlations for U-Pb Geochronology Using ^{205}Pb-^{235}U-(^{233}U)-Spiked Isotope Dilution Thermal Ionization Mass Spectrometric Data. Gechemistry Geophysics Geosystems, Q08006. https://doi.org/10.1029/2006GC001492.

Spötl, C., Mangini, A., 2007. Speleothems and paleoglaciers. Earth Planet. Sci. Lett. 254: 323–331. https://doi.org/10.1016/j.epsl.2006.11.041.

Spötl, C., Vennemann, T.W., 2003. Continuous-flow isotope ratio mass spectrometric analysis of carbonate minerals. Rapid Commun. Mass Spectrom. 17:1004–1006. https://doi.org/10.1002/rcm.1010.

Spötl, C., Offenbecher, K.-H., Boch, R., Meyer, M., Mangini, A., Kramers, J., Pavuza, R., 2007. Tropfstein-Forschung in österreichischen Höhlen – ein Überblick. Jahrb. Geol. Bundesanst. 147:117–167. http://www.zobodat.at/pdf/JbGeolReichsanst_147_0117-0167.pdf.

Sternai, P., Herman, F., Champagnac, J.D., Fox, M.R., Salcher, B., Willett, S.D., 2012. Pre-glacial topography of the European Alps. Geology 40:1067–1070. https://doi.org/10.1130/G33540.1.

Stone, J.O., 2000. Air pressure and cosmogenic isotope production. J. Geophys. Res. 105: 23753–23759. https://doi.org/10.1029/2000JB900181.

Tollmann, A., 1968. Die paläogeographische, paläomorphologische und morphologische Entwicklung der Ostalpen. Mitteilung Österreichische Geographische Gesellschaft 110, 224–244.
Wagner, T., Fritz, H., Stüwe, K., Nestroy, O., Rodnight, H., Hellstrom, J., Benischke, R., 2011. Correlations of cave levels, stream terraces and planation surfaces along the River Mur – timing of landscape evolution along the eastern margin of the Alps. Geomorphology 134:62–78. https://doi.org/10.1016/j.geomorph.2011.04.024.
Wang, X., Neubauer, F., 1998. Orogen-parallel strike-slip faults bordering metamorphic core complexes: the Salzach–Enns fault zone in the Eastern Alps. Austria. Journal of Structural Geology 20:799–818. https://doi.org/10.1016/S0191-8141(98)00013-3.
Willett, S., 2010. Late Neogene erosion of the Alps: a climate driver? Annu. Rev. Earth Planet. Sci. 38:411–437. https://doi.org/10.1146/annurev-earth-040809-152543.
Winkler-Hermaden, A., 1957. Geologisches Kräftespiel und Landformung. Springer, Vienna 822 pp.
Wisshak, M., Jantschke, H., 2010. Im Höhlenruinenniveau der Reiteralm (Berchtesgadener Alpen)? Beibelkareishöhle (1337/42) und Prünzlkopfhöhle (1337/57). Die Höhle 61: 39–47. http://www.zobodat.at/pdf/Hoehle_061_0039-0047.pdf.
Wobus, C.W., Whipple, K.X., Kirby, E., Snyder, N., Johnson, J., Spyropolou, K., Crosby, B., Sheehan, D., 2006. Tectonics from topography: procedures, promise, pitfalls. In: Willett, S., Hovius, N., Brandon, M., Fisher, D. (Eds.), Tectonics, Climate and Landscape Evolution. Geol. Soc. Amer. Special Paper. 398:pp. 55–74. https://doi.org/10.1130/2006.2398(04).
Wölfler, A., Stüwe, K., Danisík, M., Evans, N.J., 2012. Low temperature thermochronology in the Eastern Alps: implications for structural and topographic evolution. Tectonophysics 541–543:1–18. https://doi.org/10.1016/j.tecto.2012.03.016.
Woodhead, J.D., Hellstrom, J.H., Maas, R., Drysdale, R., Zanchetta, G., Devine, P., Taylor, E., 2006. U-Pb geochronology of speleothems by MC-ICPMS. Quat. Geochronol. 1: 208–221. https://doi.org/10.1016/j.quageo.2006.08.002.
Woodhead, J., Hellstrom, J., Pickering, R., Drysdale, R., Paul, B., Bajo, P., 2012. U and Pb variability in older speleothems and strategies for their chronology. Quat. Geochronol. 14:105–113. https://doi.org/10.1016/j.quageo.2012.02.028.